Available online at www.sciencedirect.com
SciVerse ScienceDirect
Journal of Hydro-environment Research xx (2012) 1–13
Journal of Hydro-environment Research
www.elsevier.com/locate/jher

Research paper

Surface discharge of negatively buoyant effluent in unstratified stagnant water

O. Abessi [a], M. Saeedi [b,*], T. Bleninger [c], M. Davidson [d]

[a] Department of Water and Environmental Engineering, School of Civil Engineering, Iran University of Science and Technology, Tehran, Iran
[b] Environmental Research Laboratory, Department of Water and Environmental Engineering, School of Civil Engineering, Iran University of Science and Technology, PO Box 16765-163, Tehran, Iran
[c] Department of Hydraulics and Sanitary Engineering (DHS), Federal University of Paraná (UFPR), Curitiba, Parana, Brazil
[d] Department of Civil Engineering, University of Canterbury, Christchurch, New Zealand

Received 1 April 2011; revised 4 May 2012; accepted 8 May 2012

Abstract

A series of laboratory experiments have been conducted for negatively buoyant effluents discharged through a protruding surface channel into unstratified stagnant water. The mixing behavior of the flow has been analyzed using digital video recordings of the dye colored discharge together with micro conductivity probe measurements. Plume trajectories and geometries have been determined by image processing and dilutions from the conductivity probe data. Comparison of non-dimensional results for plume characteristics showed similar features to those of submerged positively buoyant jets. However, notable differences are observed in the flow behavior prior to it plunging away from the free surface. As expected the overall dilution is lower when compared to submerged discharges. These differences are quantified and the new results provide information that can be used for the preliminary design of dense surface discharges.

Keywords: Dense jet; Brine disposal; Desalination; Dilution; Surface discharge

1. Introduction

Disposal of effluents with higher density than the receiving water, such as the brine (or concentrate) produced as a byproduct of the reverse osmosis process in seawater desalination plants, have recently increased; particularly in the Middle East (Safrai and Zask, 2008; Purnama and Al-Barwani, 2004). If disposed to the sea, the dense brine sinks towards the sea floor and spreads over the bed, where it may cause environmental impacts on local benthic communities. These impacts are mainly related to high salt concentrations, but are also related to chemical additives introduced to improve the desalination process (Lattemann and Hopner, 2008; Bleninger et al., 2010). The potential impacts associated with the construction and operation of seawater desalination plants, particularly large-scale facilities, are of increasing public concern (Einav and Lokiec, 2003; Lattemann and Hopner, 2003; Hashim and Hajjaj, 2005). When assessing the potential environmental impacts of brine discharges from such facilities, it is essential to have a sound understanding of the transport and mixing behavior of the effluent in the receiving water body, so that the substance concentrations and their distribution (geometrical plume properties) can be predicted with some confidence.

Surface discharges, in the form of open channel effluent releases with free surface (Fig. 1), are still a common and a very cost effective method for the disposal of large volumes of effluent into the sea (Jones et al., 2007, 1996; Doneker and Jirka, 1997). This is despite the fact that such discharges are

* Corresponding author. Tel.: +98 9121900228; fax: +98 (021)77240398.
E-mail addresses: Abessi@iust.ac.ir (O. Abessi), Msaeedi@iust.ac.ir (M. Saeedi), Tobias.dhs@ufpr.br (T. Bleninger), Mark.davidson@canterbury.ac.nz (M. Davidson).

1570-6443/$ - see front matter

Please cite this article in press as: Abessi, O., et al., Surface discharge of negatively buoyant effluent in unstratified stagnant water, Journal of Hydro-environment Research (2012), doi:10.1016/j.jher.2012.05.004

Fig. 1. Surface protruding discharge, the open channel effluent in Hesham power station outfall, United Kingdom.

less efficient in terms of mixing and entrainment. Their impact on the associated coastal zone is also more significant because much of the required infrastructure is above ground. However, the cost of submerged discharges from large desalination plants (with low recovery rates), where effluent flows are very large (5 m^3/s), can be prohibitive, hence many desalination plants still employ shoreline channels to discharge their brine effluent into the near shore zone (Ahmed et al., 2001; Lattemann and Hopner, 2008). Nevertheless, surface discharges are usually not recommended in sensitive coastal regions, due to their proximity to the coastline and near shore habitats, and the associated reduced mixing efficiency. A compromise solution is presented here using protruding channel configurations, reducing direct shoreline impacts and enhancing the initial mixing characteristics (Fig. 1). The present study investigates the prediction of concentration distributions for those discharges, which are then compared to submerged discharge configurations (Bleninger and Jirka, 2008) providing a framework for assessing these alternative discharge configurations.

Submerged brine discharges in stagnant waters (not discharging at the surface, but through a pipe near the seabed), have been studied more intensively in recent years and are designed to create a rising plume, which then falls back to the seabed without interaction with the free surface. Previous studies are generally of an experimental nature and cover a variety of discharge configurations, for example submerged vertical discharges (Turner, 1966; James et al., 1983; McLellan and Randall, 1986; Baines et al., 1990; Zhang and Baddour, 1998), and inclined dense discharges (Zeitoun et al., 1972; Roberts et al., 1997; Cipollina et al., 2005; Kikkert et al., 2007). These studies have mostly focused on the determination of key flow characteristics in stagnant waters.

In contrast, dense *surface discharges* have not been studied to the same extent. These discharges create a jet moving along the sea surface and then plunging down to the seabed in the form of a negatively buoyant jet flow. Once reaching the bed the impinging jet forms a density current along the bed. Key parameters involved in the characterization of dense surface discharges in stagnant environments are schematized in Fig. 2. An off-shore protruding discharge without a solid vertical boundary below the channel (the channel is built on piles) is shown in this figure. The pile construction allows the jet to entrain fluid from below without attaching to a boundary. Provided that the distance to the shoreline and ambient depth are large enough that boundary conditions do not affect the flow mixing process. In this paper it is assumed that these values are sufficiently large that the discharge fluid is able to fall freely without the influence of these parameters. Further studies are planned where these potential boundary influences will be incorporated. The Cartesian coordinate system in Figs. 2 and 3 is defined such that the positive x direction is oriented in the direction of the jet, z vertically downwards, along gravity, and y is perpendicular to x–z plane, with the origin in the middle of the discharge on the water surface. The discharge channel depth is represented by h_0 and its width b_0.

The horizontal progress of the surface region is due to the initial momentum flux $M_0 = Q_0.U_0$, where U_0 denotes the initial discharge velocity, and $Q_0 = U_0.b_0.h_0$ the initial flow rate. After reaching a terminal length adjacent to water surface (x_p), the flow plunges into deeper parts and forms a progressive submerged plume due to the buoyancy flux ($B_0 = g'.Q_0$, $g' = \frac{\rho_0 - \rho_a}{\rho_a} g$, where g' is initial reduced gravity term, g is acceleration due to gravity, ρ_0 denotes the initial effluent density, and ρ_a the uniform ambient density). The plume then impinges on the sea floor at x_i and spreads as a density current in all directions. x_m and S_m also denote the location and dilution at the point of ultimate dilution, which will be discussed subsequently.

A significant number of studies in the past have focused on the *surface discharge of positive buoyant effluents* (Jones et al., 2007; Jirka, 2007; Amon and Benner, 1998; Nash and Jirka, 1996; Chu and Jirka, 1986; Wright, 1984; Abdelwahed and Chu, 1981; Jirka et al., 1981), which have different flow features that those of dense surface discharges. There are only few investigations of non-buoyant or negatively-buoyant flows (Law et al., 2004; Gholamreza-Kashi et al., 2007; Kassem et al., 2003). As noted above, disposing of an effluent with larger density than the ambient water, the inflow plunges and forms a density underflow. Kassem et al. (2003) carried out analytical and experimental studies in order to characterize *density currents* in diverging channels. The development mechanisms of negatively buoyant flows in diverging channels with a sloping bottom were investigated. Different divergence angles and inflow densimetric Froude numbers were employed to investigate distinct flow regimes with various cases of plunging and associated density currents.

Laboratory studies of the initial flow field characteristics of a *neutrally buoyant rectangular surface jet* were carried out by Gholamreza-Kashi et al. (2007) and in double-diffusive form by Law et al. (2004). Gholamreza-Kashi et al. (2007) studied the flow turbulence development of a non-buoyant rectangular surface jet and measured the jet lateral and vertical growth rates. The horizontal and vertical profiles of the velocity were

Please cite this article in press as: Abessi, O., et al., Surface discharge of negatively buoyant effluent in unstratified stagnant water, Journal of Hydro-environment Research (2012), doi:10.1016/j.jher.2012.05.004

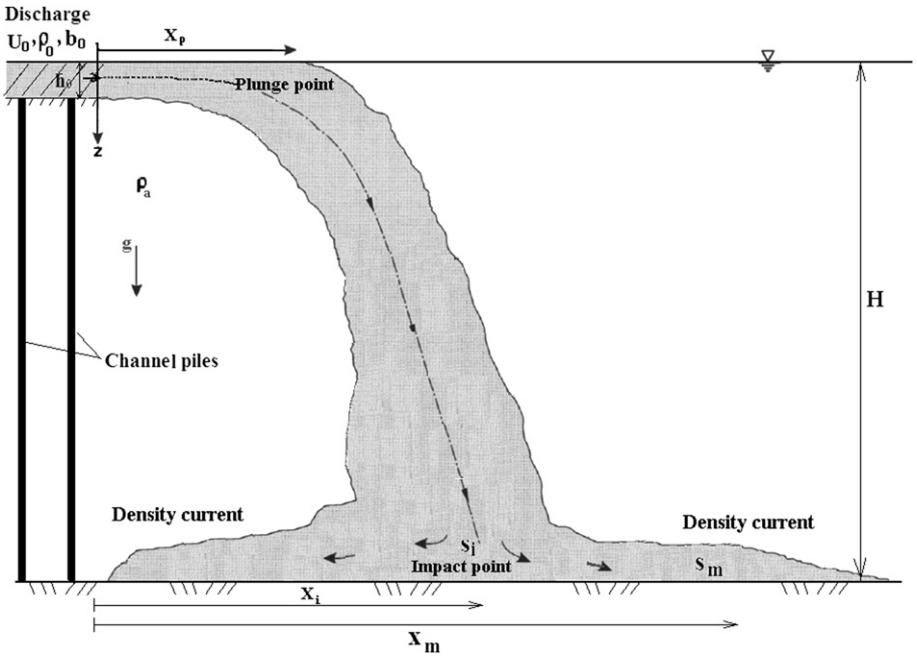

Fig. 2. Schematic view of dense protruding surface discharge in stagnant environment, channel is mounted on piles and jet free-falls to a horizontal sea-bed.

also compared with those observed in free, submerged, and wall jets. Law et al. (2004) studied the behavior of a double-diffusive neutrally buoyant surface discharge. They characterized the effect of salt-fingering on jet surface propagation and showed the jet plunged downward towards the bottom at a distance of approximately $x/D_0 = 6$ (where D_0 is the channel equivalent diameter). No specific laboratory study has reported on flow behavior for *negatively buoyant surface jets.*

In the present study, laboratory experiments have been developed using digital video technology. The objective of the study is to define trajectory and geometric properties of negatively buoyant surface discharges released into a stagnant ambient including important flow characteristics such as the plunging point and the impingement point. Besides flow geometries, the data from the experiments provide additional information about flow mixing and dilution characteristics. The decay of centerline light intensity, centerline dilution, dilution at impact point and flow ultimate dilution are also measured.

2. Dimensional analysis

The features of turbulent buoyant jets are characterized by source fluxes, the discharge volume flux, momentum flux and buoyancy flux (Fischer et al., 1979). When the open channel flow is fully turbulent (initial Reynolds number $Re_0 = U_0.h_0/\nu > 500$) and the effects of molecular viscosity are negligible, any dependent properties of the flow in stagnant water, can be expressed as:

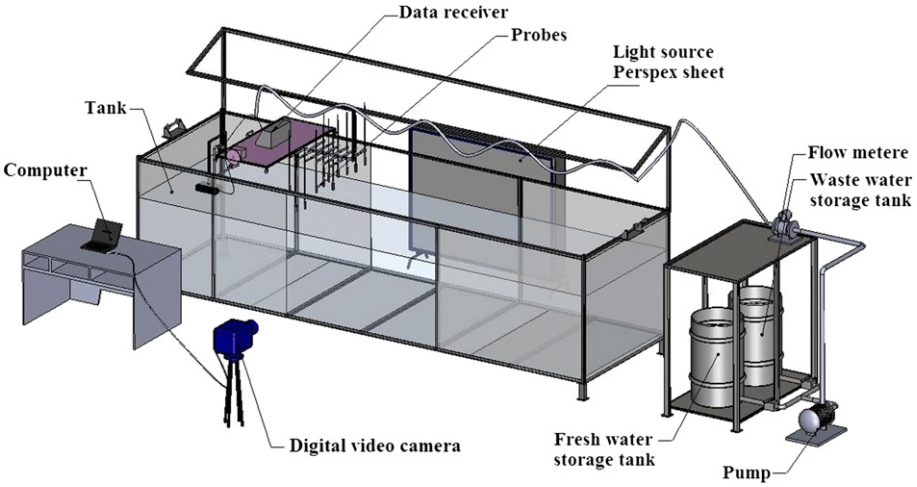

Fig. 3. Schematic diagram of experimental setup.

Please cite this article in press as: Abessi, O., et al., Surface discharge of negatively buoyant effluent in unstratified stagnant water, Journal of Hydro-environment Research (2012), doi:10.1016/j.jher.2012.05.004

$$\text{Jet property} = (Q_0, M_0, B_0, H, h_0, b_0, x, y, z) \quad (1)$$

where M_0 is flow initial momentum flux ($M_0 = Q_0.U_0$), Q_0 is initial flow rate ($Q_0 = U_0.b_0.h_0$), B_0 is buoyancy flux ($B_0 = g'.Q_0$), H is ambient water depth, h_0 and b_0 are flow depth and width in the channel and x, y, z are the Cartesian coordinates. Using dimensional analysis, flow mixing properties can be correlated to the jet initial fluxes and discharge characteristics. Making use of these fluxes and dimensional arguments, the discharge length scale (L_Q) and jet to plume length scale (L_M) have previously been defined and employed to characterize the properties of buoyant jet flows (examples include Wright, 1984; Roberts and Tom, 1987; Jirka, 2004; Bleninger and Jirka, 2008; Jirka, 2008).

$$L_Q = \frac{Q_0}{M_0^{1/2}}; \quad (2)$$

$$L_M = \frac{M_0^{3/4}}{B_0^{1/2}} \quad (3)$$

The discharge length scale (L_Q) represents the relative importance of the volume flux to momentum flux and defines the region where the discharge geometry strongly influences the flow properties. The jet to plume length scale (L_M) represents the relative importance of the initial momentum flux to the initial buoyancy flux and indicates the location where buoyancy flux has a more dominant influence than the initial momentum flux. The ratio of these two length scales can be expressed as the densimetric Froude number ($Fr_d = u_0/\sqrt{g'.h_0}$). For distances from the discharge point greater than L_Q, initial volume flux becomes dynamically unimportant and L_Q drops out from the influential parameters. Thus, based on dimensional analysis, any dependent variable in Equation (1) can be written as a function of the dimensionless parameters as follows (Fischer et al., 1979; Jones et al., 1996):

$$\text{Dimensionless jet parameter} = f\left(\frac{H}{L_M}, \frac{x}{L_M}, \frac{y}{L_M}, \frac{z}{L_M}, \frac{h_0}{b_0}\right) \quad (4)$$

In this relationship, the dimensionless jet parameter can be geometric (χ/L_M) or normalized dilution (S/Fr_d) following the likes of Roberts et al. (1997), Jirka (2004) and Bleninger and Jirka (2008). This approach provides a convenient framework for collapsing experimental data and making comparisons with model predictions.

3. Experimental setup and procedure

3.1. Setup

The experiments were conducted by releasing a continuous salt water flow into a glass-walled tank filled with fresh water. The tank has a length of 6 m, a width of 1.8 m and a depth of 1.5 m with fresh water depths ranging between 0.40 and 0.66 m (Fig. 2). The walls are made of 20 mm thick transparent glass. A separate storage tank with 220 L capacity was utilized as the source for the brine discharge. The discharge system released the flow at the surface through a rectangular and horizontal channel of 6.4 cm width and varying depths from 0.65 to 2.1 cm. A rotary pump was utilized to pump the brine from the storage tank to the channel and a calming device used between pipe and channel to reduce wave motions and secondary flows. To help provide a developed turbulent profile the channel was 0.8 m long. The receiving tank water level was kept constant by having an overflow weir at the end of the tank. The water level at the end of the discharge channel was regulated such that it was at the same elevation as the water level in the receiving tank.

3.2. Measurement techniques

The salinity of the effluent in the storage tank was measured using a calibrated conductivity probe. The probe was the product of Lutron company (Model: YK-2014CD) that measures conductivity in the range of 0–200 ms with the resolution equal to 0.1 ms. This probe also provides temperature measurements, which together with salinity, have been used for density computations (Millero and Poisson, 1981). An electromagnetic flow meter (WELLTECH COPA-XE WT4300) measured the flow rate in the discharging pipe. The characteristic initial discharge velocity U_0 was determined by dividing the measured flow rate by the channel water depth (h_0) and width (b_0).

A light source made of twenty-five 50 Hz–40 W fluorescent tubes (1.2 m tubes) equipped with a light diffuser (opaque plastic sheet) was placed behind the receiving tank to provide an intense, white, uniform background light source. The experiments were conducted in the dark laboratory room to avoid other light sources disturbing the experiments. A black soluble dye was used as a tracer. The dye was a conservative textile dye with similar density to water and minor influences on effluent viscosity.

For each experiment a video sequence with the frequency of 30 frames per second was recorded using a Sony DCR-SR47 digital camcorder installed on a tripod on the side of the receiving tank. The camera was placed 4 m from the tank, perpendicular to the central vertical plane of the flow.

3.3. Experimental procedure

Two series of experiments, one equipped with conductivity probes for dilution measurement and another without probes in the dark room to identify flow geometric properties, have been carried out. In the first series, 45 experiments were conducted for discharge densimetric Froude numbers ($Fr_d = U_0/\sqrt{g'.h_0}$) ranging from 2.1 to 16. The flow was fully turbulent with the channel Reynolds numbers ($Re = U_0.h_0/\nu$) in the range of 750–3300. In the second series 22 experiments were conducted, in which, discharge densimetric Froude numbers ranged from 1.82 to 11.5 and Reynolds numbers of discharge were in the range of 720–2680. Having the same source condition in both series, the effluent density ranged from 1007 to 1038 kg/m^3 with salinities from 14 to 55 ppt and

Please cite this article in press as: Abessi, O., et al., Surface discharge of negatively buoyant effluent in unstratified stagnant water, Journal of Hydro-environment Research (2012), doi:10.1016/j.jher.2012.05.004

temperatures ranging from 20 to 24 °C. The depth of ambient water was in the range of 48.9–60.8 and the density of water was changing slightly around 998.6 (998.5–998.7) kg/m^3. Therefore, the minimum and maximum density difference of 8.3 and 39.5 kg/m^3 have been investigated here.

During the tests, the dye colored salt water was discharged into the tank of fresh water at a constant flow rate and concentration. The selected parameter values are typical of those for brine discharges from desalination plants (Jirka, 2008) that were kept constant during the experiments. During each run sufficient time (20–40 s) was allowed for the flow to become established, after which video sequences (50–90 s) were recorded or conductivity measurements made.

4. Analysis

4.1. Processing of images

To analyze the video sequence from the dye experiments, 1500–2700 frames were exported and time averaged using the Image Stream software (Nokes, 2008). The IrfanView (http://www.irfanview.com) image software was used in batch mode to convert all average pictures from the different experiments into inverted gray scale images in which the light intensity of each pixel ranges from 0 to 255 with minimum for pure white and maximum of pure black. The gray scale image provided a manageable volume of data for each experiment.

For image post processing, the light intensity of each pixel of the averaged-gray scaled pictures was digitally analyzed using an in-house MatLab script (using MatLab *Ver. 6*, http://www.mathworks.com). The image was represented as a matrix of intensity values $I(i,j)$ for each pixel in line i and column j. The dye field light intensity in various sections was processed further to find the flow trajectory, the jet cross sectional profiles, the plume width, and the plunging and impact point locations.

As, the vertical motion of these flows was generally significant, it was possible to obtain a reasonable estimate of the location of the flow centerline by analyzing horizontal lines (i) for maximum light intensity. The jet trajectory was determined by connecting these points. The jet normal cross sectional profiles were extracted using the following procedure coded in MatLab: (i) The light intensity profiles were plotted for several cross sections perpendicular to the trajectory, (ii) The light intensities, $I(i,j)$, were normalized with the centerline maximum intensity, $I_{max}(i,j)$, iii) the width b_v was defined by finding distance r from the centerline on the vertical plane, where $I = I_{max}.e^{-1}$, iv) the profiles were then plotted in normalized form as I/I_{max} and r/b_v.

Light intensities along horizontal lines adjacent to the surface were analyzed to identify the plunging point location. The location where the jet leaves the ambient surface was selected as the plunging point of the flow. The impingement point on the bed was also defined where the jet trajectory hits the bed. Similar light based techniques have been employed by Zhang and Chu (2003), Kikkert et al. (2007) and Bandas et al. (2008). Although the setup is relatively simple and inexpensive, results show good agreement with more sophisticated experiments.

4.2. Dilution measurements

The corresponding dilution at jet impingement and the ultimate jet dilution were determined by analyzing the results of 20 conductivity probes (Lutron YK-2014CD, same probe describe above) placed at the impact point and in the region surrounding it. Knowing the conductivity, dilution was measured by $S = \frac{C_0 - C_a}{C - C_a}$ where C, C_0 and C_a are conductivity at sampling point, effluent source and ambient water, respectively. In addition, dilutions were measured along the trajectory by locating the probes along the previously determined jet centerline. The conductivity of points was the normal average of probe measurements for the time period of experiments.

5. Results and discussion

5.1. Cross sectional profiles

As indicated above in order to analyze the intensity distribution, the cross sectional profiles at various locations perpendicular to the centerline were extracted. Fig. 4 shows image and intensity contours of a discharge with $Fr_d = 2.27$ in the ambient with 60.8 cm depth. Dark zones of the right image in Fig. 4 show areas with high intensity of black dye, bright zones show lower intensities. The left image shows iso-intensity contours of the same image. In the figure, dotted lines are the approximate position of cross sections along flow centerline where z is coordinate of vertical axis and b_0 is channel width. Fig. 5 presents the intensity profiles of these cross sections perpendicular to the trajectory of the flow. In this figure r is distance perpendicular to flow path in the x–z plane with the sectorial orientation from outer to inner side of the flow. The profiles generally exhibit a good axisymmetric self-similar Gaussian pattern. However, an increasing deviation from this axisymmetric pattern is noted with increasing vertical distance from the source (increasing z/b_0).

The distortion of the inner side of profiles has formerly been reported for submerged negatively buoyant discharges by Kikkert et al. (2007) and Shao and Law (2010). Kikkert et al. (2007) reported that the jet is initially Gaussian in the inner side of plume, but this becomes increasingly distorted due to the presence of buoyancy-driven instabilities. In both studies the expansion of inner mean cross sectional profiles was highlighted. Similar features are observed for negatively buoyant surface discharges, where the distortion is consistent with profiles from submerged horizontal axisymmetric discharges presented in Kikkert (2006). It is evident that the buoyancy-driven instabilities generate additional mixing on the inner side of the surface discharge, which enhances the flow dilution at this region.

5.2. Jet trajectory

The jet trajectories have been measured for a range of initial densimetric Froude numbers, through variations of discharge velocities and/or density differences. Fig. 6 presents

Please cite this article in press as: Abessi, O., et al., Surface discharge of negatively buoyant effluent in unstratified stagnant water, Journal of Hydro-environment Research (2012), doi:10.1016/j.jher.2012.05.004

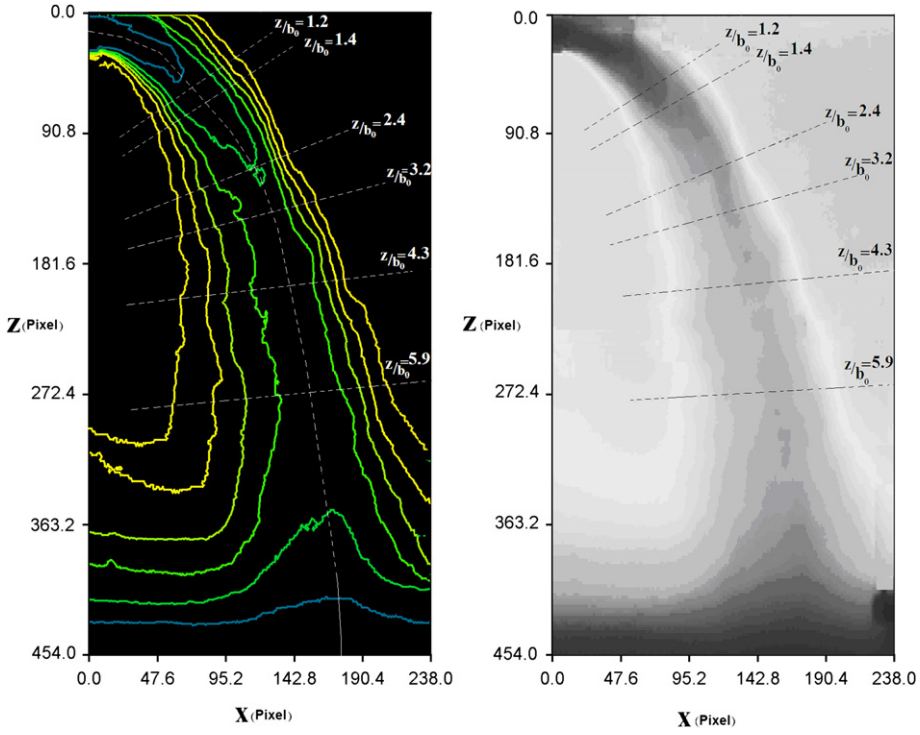

Fig. 4. Iso-intensity photo of flow path in surface discharge of negatively buoyant jet.

the trajectories of all experiments, normalized with L_M. The trajectories collapse as expected and are almost identical to experimental data from submerged horizontal buoyant jet discharges (Fan, 1967; Hansen and Schroder, 1968; Davidson and Pun, 2000; Xiao et al., 2009).

Results are also compared with the standard jet integral model CorJet (Jirka, 2004). The model has been extensively validated and is arguably the most thoroughly validated of the standard integral solutions. CorJet models submerged jets, assuming unlimited ambient water, and hence does not specifically include surface discharge effects. However, this model is also embedded within the CORMIX expert system which allows for the prediction of not only the buoyant jet phase, but also of other mixing processes, such as the formation of the bottom density currents, boundary interactions and transitions to far-field mixing. Here CorJet has been applied to simulate the surface discharge experiment as a submerged buoyant discharge with identical fluxes and flow orientation. Of course discrepancies are expected due to the missing surface effect. In addition, CORMIX1 simulations are also presented, where the surface discharge effects are taken into account. Fig. 6 contains the normalized prediction of both models, which collapse on obtained data and show good agreement with the measured data and the literature values. In

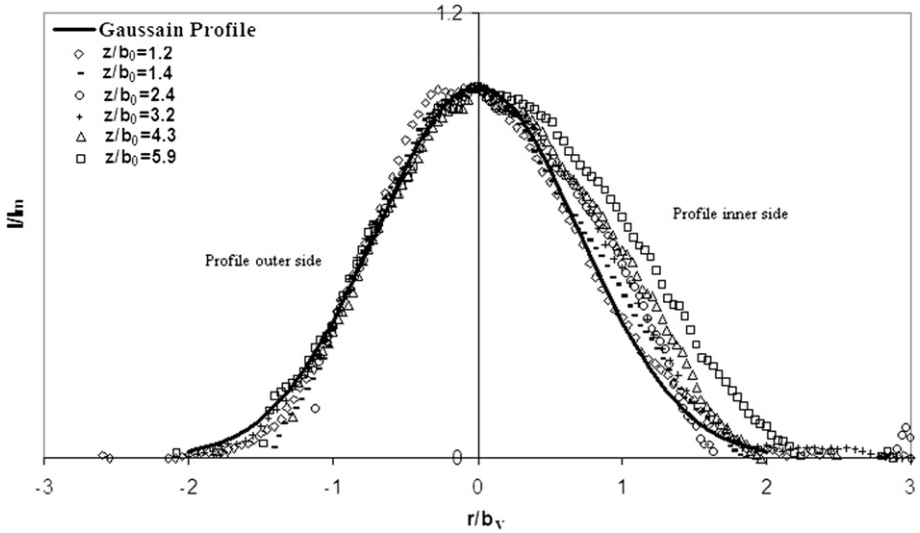

Fig. 5. The cross sectional profile at various downstream distances in an experiment with $Q_0 = 287$ cm^3/s, $\Delta\rho = 0.039$ gr/cm^3, $Fr_d = 3.27$.

Please cite this article in press as: Abessi, O., et al., Surface discharge of negatively buoyant effluent in unstratified stagnant water, Journal of Hydro-environment Research (2012), doi:10.1016/j.jher.2012.05.004

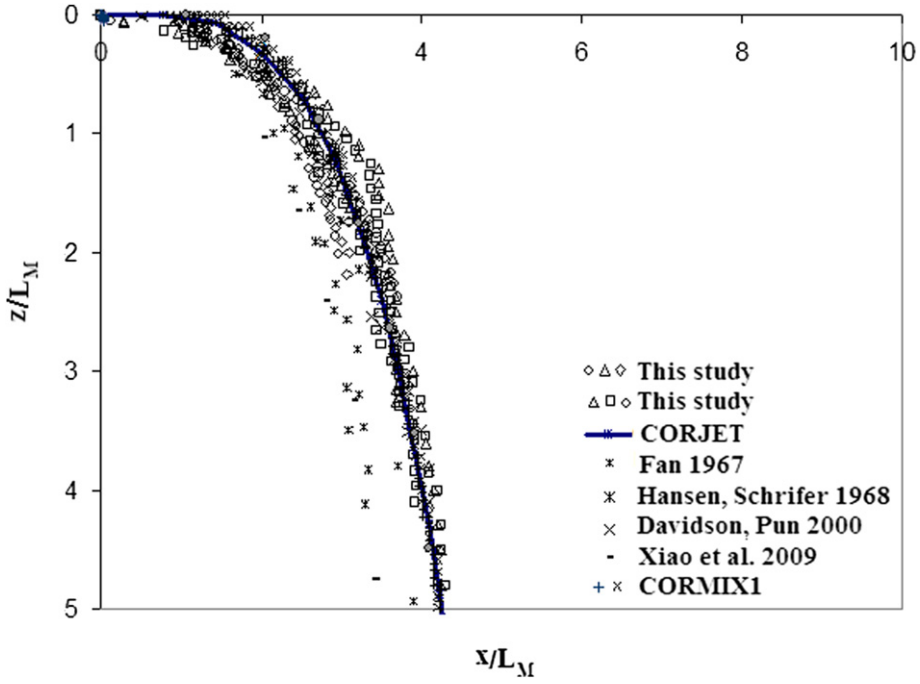

Fig. 6. Normalized jet centerline trajectory for negatively buoyant surface jet discharges into stagnant ambient.

this figure flow trajectories obtained from the experiments, and the results of CORJET and CORMIX predictions, did not show any additional dependence on densimetric Froude number for the investigated range of initial conditions ($Fr_d = 2-16$).

The consistency of the data presented in Fig. 6 indicates that the simple measurement and analysis technique applied here is capable of capturing the major features of interest for these flows. Furthermore, the results indicate only small differences in trajectory between submerged and surface discharges in the initial part of flow. The flow trajectory of surface jets protrudes farther along close to surface, before diving downwards. This is due to the influences of the surface boundary, which cause dynamic attachment of the discharged jet to the free surface.

5.3. Jet width

The jet width is usually defined as the distance from the jet centerline where the intensity value is $1/e$ of the centerline value, thus $I(b_v) = 1/e.I_{max} = 0.37\ I_{max}$ (Jirka, 2006). The width development (b_v) along the trajectory is plotted in Fig. 7, normalized by L_M. For comparison, again predictions by CorJet and CORMIX1, and an empirical relation defined by Jirka (2004) ($b_v = 0.12\ z$) are also presented. Note the CORMIX1 predictions are relatively low resolution because the software is designed for predicting full scale flow. As depicted in this figure the results show general linear rate of increase of jet width in vertical direction without dependence on densimetric Froude number for the range of initial conditions investigated. The negatively buoyant surface discharge

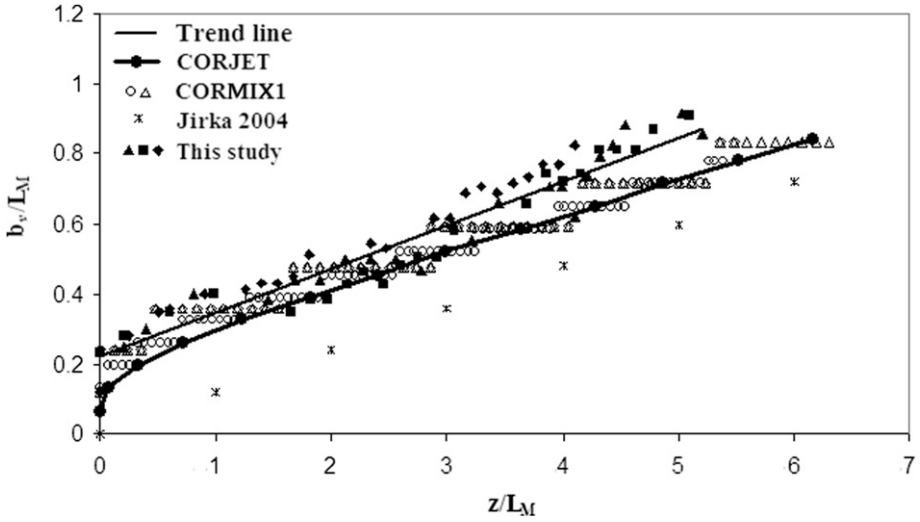

Fig. 7. Changes of flow width (b_v) along the jet vertical trajectory.

Please cite this article in press as: Abessi, O., et al., Surface discharge of negatively buoyant effluent in unstratified stagnant water, Journal of Hydro-environment Research (2012), doi:10.1016/j.jher.2012.05.004

experiments showed relatively the same growth rate when compared to the submerged jet results. It is evident that in surface dense discharges the influence of free surface on the entrainment and mixing and hence the growth rate of the flows is small.

5.4. Centerline dilution

The centerline dilution has been measured by two different methods. Firstly by analyzing the light intensity distributions and secondly by analysis of recordings of conductivity probes along the jet centerline. As previously mentioned mean concentration distributions, along the flow path, are commonly assumed to be Gaussian, therefore, an integrated Gaussian profile in the y direction is observed with the light intensity method. Bulk parameters, including peak integrated dilutions, are determined from these integrated profiles based on the Gaussian assumption. Herein, decays of centerline light intensity (I_c/I_{max}) were calculated by finding point intensity values from the integrated values. The process is discussed in more detail in Kikkert (2006). Fig. 8 shows the results for the light intensity distribution analysis. This figure shows the decay of centerline black dye intensity (I_c/I_{max}) as a function of horizontal distance to channel depth (x/h_0) with data from different experiments. The ZFE can be clearly seen at about x/h_0 of 6, showing constant intensity in the jet centerline, until the shear zone reaches the centerline location. Beyond this the centerline intensity (I_c) starts to decrease due to entrainment and mixing. The experimental results are consistent with CorJet, the analytical theory (Lee and Chu, 2003) and literature values (Albertson et al., 1949; Rosler and Backoff, 1963; Capp, 1983; Wang and Law, 2002) regarding the potential core length of 6 diameters. Interestingly the discharge geometries for the present experiments were not axisymmetric and b_0 ranged from $3h_0$ to $10h_0$. However these differences in discharge geometry and the presence of the free surface do not appear to have had a noticeable influence on the length of the potential core. In contrast the results indicate relatively low values of dilution for these discharges, due to the effects of ambient surface interaction.

The accuracy of the light intensity distributions depends on image resolutions, in regions with high gradients. High gradients are expected very close to the discharge channel, where the image processing technique is not capable to resolve and to detect the initial light intensity accurately. This influences the determination of the initial absolute value I_{max} used for the normalization. Therefore, further experiments have been conducted using conductivity probes located along the jet trajectory. The decrease of conductivity was calculated by measuring it in different points along the centerline trajectory (C_c) and its ratio to source flow conductivity (C_c/C_{max}). The results of conductivity probes were plotted in Fig. 8 together with the data achieved for decay of centerline light intensity. The results of probes and light intensity analysis are coincident and both are close to data previously reported.

Based on conductivity probe data, Fig. 9 shows the centerline dilution (S) along the vertical coordinate z, together with results from laboratory studies of Hansen and Schroder (1968), Liseth (1970) and Xiao et al. (2009), and prediction of CORMIX model for a horizontal submerged buoyant discharge. The dilution has been normalized by the densimetric Froude number, and the geometric values using L_M. The results show a similar behavior for the different studies with no additional dependence to densimetric Froude number for the observed range in the experiments. However, dilutions are generally lower (40–70%) than for the submerged jet cases, due to the interactions with the surface and thus limited mixing.

5.5. Plunging point

The point where the jet departs from the surface is defined as the plunging point. The values of the plunging point locations were derived from digital processing of experiments. The plunging point has been defined at the location, where the light intensity gradient in surface pixels decreases sharply in the horizontal direction. In Fig. 10 the horizontal distance to the

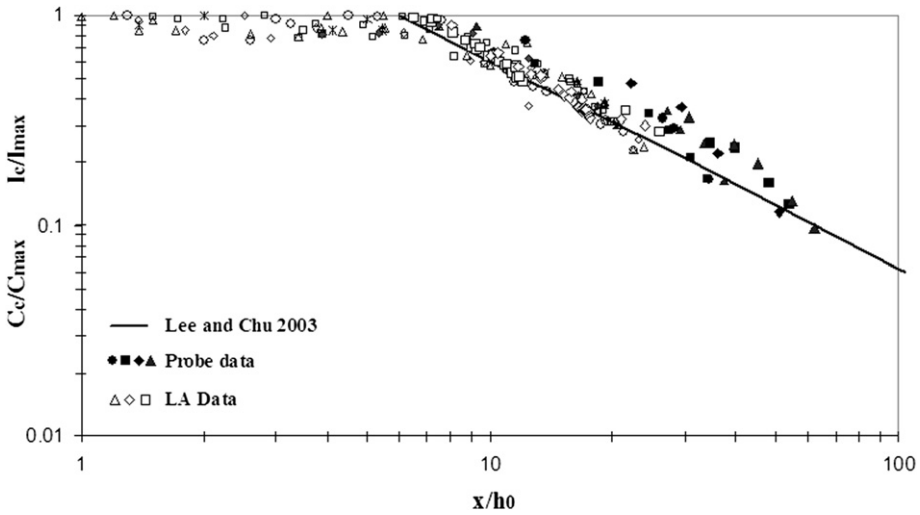

Fig. 8. Decrease of centerline conductivity (C_c) and centerline light intensity (I_c) decay along the jet trajectory (x).

Please cite this article in press as: Abessi, O., et al., Surface discharge of negatively buoyant effluent in unstratified stagnant water, Journal of Hydro-environment Research (2012), doi:10.1016/j.jher.2012.05.004

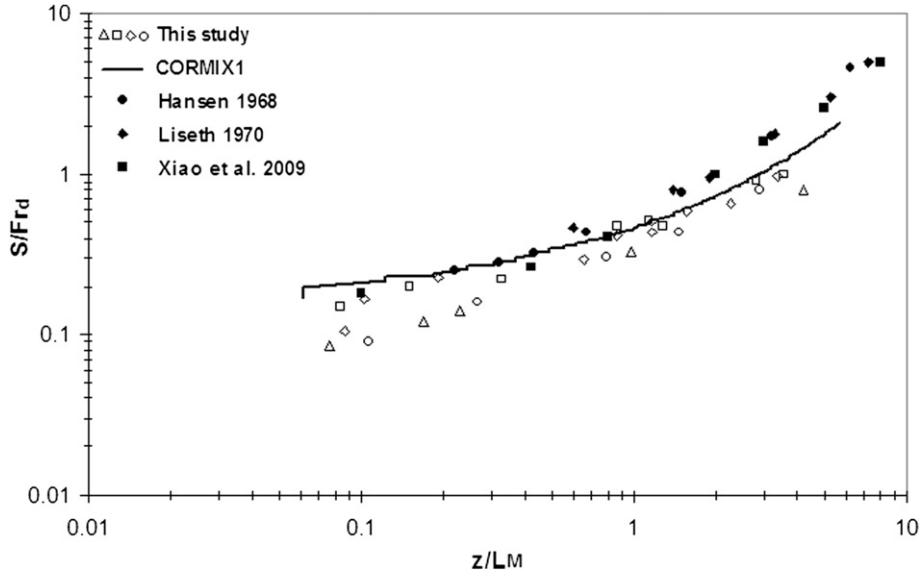

Fig. 9. Normalized centerline dilution S/Fr_d against vertical level below the water surface z/L_M.

plunge point (x_p) is plotted against the jet to plume length scale (L_M) both normalized by L_Q. Data from Sharp and Vyas (1977) has been added for comparison. Their data was obtained from a set of experiments where positively buoyant jets were released along a solid boundary. This experimental configuration is equivalent to that of the present study, if the shear stress from the solid boundary does not have a significant influence on the horizontal momentum flux of the flow (before it detaches from the bottom boundary). The consistency between the data sets suggests that this was the case. In Fig. 10 the location of plunge point is described by $x_p/L_Q = \alpha_p.(L_M/L_Q)$ and α_p is approximately equal to unity for the experiments. This suggests in surface discharge of dense jets the flow plunges prior to the jet to plume transition. Proximity of the results with Sharp and Vyas's study shows the similarity of flow in these two conditions.

5.6. Impact point

The location where the jet impinges on the bed is defined as the impact point. Environmental impact studies often need to evaluate the concentration at this location in comparison with benthic habitat sensitivity. Fig. 11 shows the horizontal location of the impingement point, x_i, plotted against the water depth H and both are normalized with L_M. In the experiments, the ratio of $\frac{H}{L_M}$ changed in the range of 2.6–9.1 and $\frac{h_0}{H}$ from 26 to 70. The results indicate that the horizontal impingement distance is dependent on the jet to plume length scale and water depth. This of course is only true for discharges in deep waters where $H >> L_M$, so that a plume is able to form and the flow is then predominantly in the vertical direction. As depicted in Fig. 6, when the water depth becomes large the

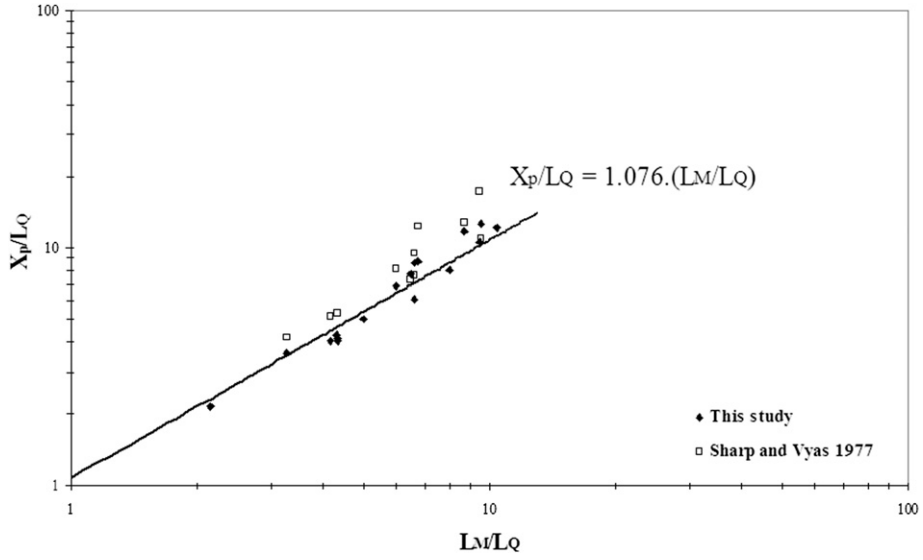

Fig. 10. The horizontal distance of plunge point.

Please cite this article in press as: Abessi, O., et al., Surface discharge of negatively buoyant effluent in unstratified stagnant water, Journal of Hydro-environment Research (2012), doi:10.1016/j.jher.2012.05.004

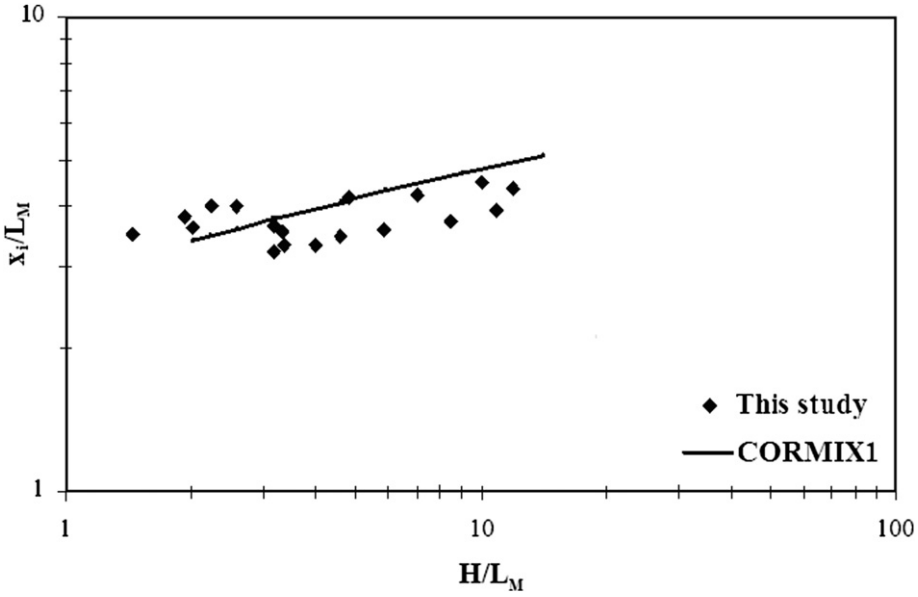

Fig. 11. The horizontal distance of impingement point.

flow trajectory becomes essentially vertical and jet impact point appears to approach an asymptotic value.

The jet impingement on the bed creates additional flow features, boundary mixing and spreading. This inhibits the determination of dilution values using the image processing technique. Therefore, again conductivity probe results have been used. The probes were located at the position of the impingement point and the measured dilution (S_i) is normalized by the initial densimetric Froude number (S_i/Fr_d) and plotted against $\frac{H}{L_M}$ in Fig. 12. CORMIX1 (submerged horizontal buoyant jet) predictions for flow dilution at the location of impact point (interaction with a surface) were also plotted. As shown in this figure, dilution at impact point is a function of $\frac{H}{L_M}$ which means it changes continually with variation of ambient depth (H) and the initial discharge parameters (L_M, Fr_d). The data in this figure is showing surface discharges in deeper waters provide higher dilution as expected.

5.7. End of initial mixing

When the jet impinges on the bed, the flow undergoes fast lateral expansion and forms a density current moving along the floor. In this region, the flow trajectory is direct function of the local bathymetry, the bottom slope and the ambient density structure. Jet mixing, impingement and spreading processes are commonly considered as the initial mixing region. The

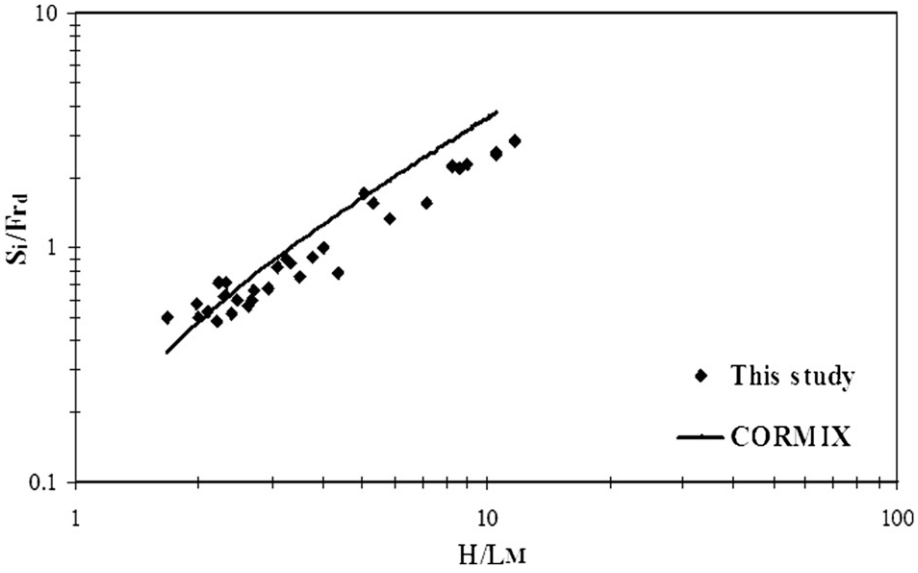

Fig. 12. Dilution of jet centerline at impact point.

Please cite this article in press as: Abessi, O., et al., Surface discharge of negatively buoyant effluent in unstratified stagnant water, Journal of Hydro-environment Research (2012), doi:10.1016/j.jher.2012.05.004

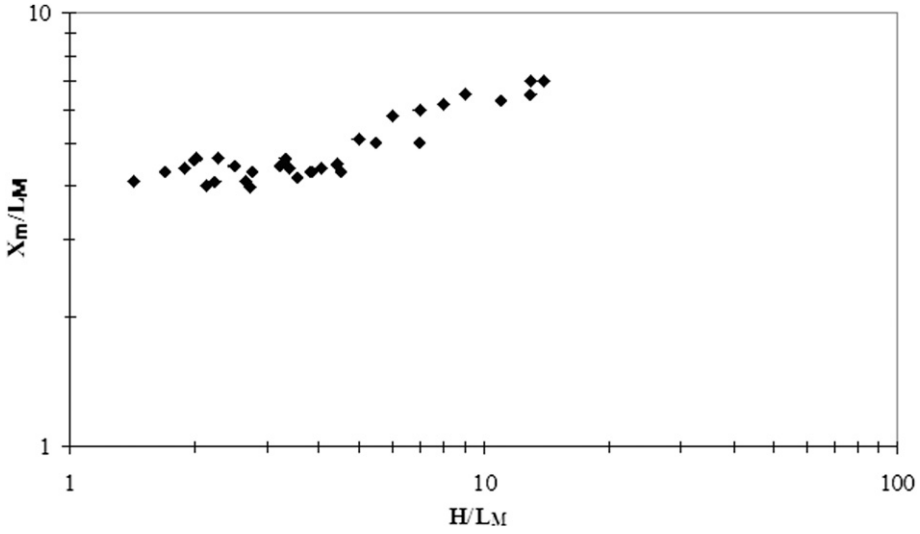

Fig. 13. The variation of location of ultimate dilution with the ambient water depth in surface discharges of negatively buoyant jets.

near-field ends at the impingement point. The intermediate-field includes the boundary interaction processes. The established final density current denotes the far-field region, where mixing processes are relatively low. Detail process descriptions of this region have been formerly described by Roberts et al. (1997). They assumed that initial mixing ceased where the discharge induced fluctuations collapse or the point where flow concentration has no significant change along the trajectory in x direction. This point defines as the end of the initial mixing region, x_m.

The results of conductivity probe measurements have been used to determine the location of this point. Given the experimental tank width was limited to 1.8 m, data gathered within the boundary interaction region was eventually influenced by the reflection of the associated gravity current from the sidewalls. The influences of these reflections were seen in the time series obtained from the conductivity probes, where the initial steady state value changed slightly as reflected material returned to the flow centerline. In all reported experiments the distance between jet impact point (x_i) and the location of ultimate dilution (x_m), $x_m - x_i$, is less than $2x_b$, the distance where the boundaries of the dense plume reach the sidewalls (x_b) and reflected back to centerline. Thus the influence of the sidewalls was avoided by using data from the initial steady regime in the time series.

Making use of the conductivity probes, the location (x_m) has been obtained by determining the point where the mean conductivity no longer changes along the bed. Results have been normalized by L_M, and plotted in Fig. 13 for a horizontal bed. Axial dilution values at this location (S_m/Fr_d) are also

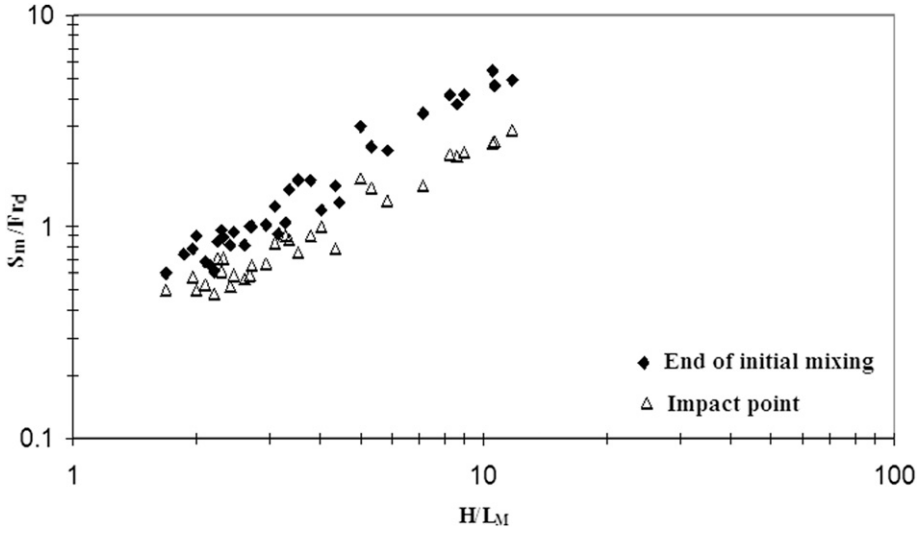

Fig. 14. The variation of dilution at the end of the initial mixing zone and impact point with the ambient water depth in surface discharges of negatively buoyant jets.

Please cite this article in press as: Abessi, O., et al., Surface discharge of negatively buoyant effluent in unstratified stagnant water, Journal of Hydro-environment Research (2012), doi:10.1016/j.jher.2012.05.004

plotted in Fig. 13 against the normalized depth (H/L_M). As depicted ultimate dilution of flow is 40–50% higher than at the impact point. In Fig. 14 it is also clear that maximal dilution of flow changes with the variation of ambient depth (H) and initial discharge properties (L_M).

6. Conclusion

The surface discharge through an open channel of dense effluent is a very common application of desalination plant discharges into coastal waters. The design and location of such structures must include the determination of flow geometrical and mixing characteristics to enable the designer to assess the environmental impacts of the discharge for regulatory purposes. Several laboratory experiments were performed to investigate the flow behavior of surface channel discharges of dense jets in unstratified stagnant water. Results for jet trajectories and dilution have been obtained by an inexpensive measurement technique using the light intensity methodology. Light intensity distributions of the colored discharge plume have been produced by processing digital camera images of the flow field. Comparisons with more sophisticated lab studies, as well as with numerical model results, showed a good agreement for that application. The comparisons furthermore showed that the surface dense discharge generally follows similar mixing process as submerged horizontal buoyant jets. Major differences are lower jet dilutions (40–70%), due to the limited mixing processes in the initial surface interaction region. Surface interaction in the form of the flow protruding along the free surface occurred over a distance L_M and beyond this distance the flow plunged away from the free surface. Protruding dense surface discharges showed maximum dilutions at the end of jet initial mixing zone to be 40–50% higher than the impact point, both increased with ambient depth. The above information can provide some guidance in the preliminary design of protruding surface discharges.

Acknowledgment

This research was carried out under financial supports of Iran University of Science and Technology (IUST) and COE in Enviro-Hydroinformatics of IUST. The writers are very appreciative of Dr. Naser Hajizadeh-zaker assistance in doing this study and Mr. Ovais Abessi for the design of set up and his kind helps.

Notation

The following symbols are used in this paper:

A_0	flow cross section, m^2 $(=h_0.b_0)$
b_0	channel width, m
h_0	discharge depth in channel, m
H	ambient water depth, m
u_0	discharge velocity, m/s
g	acceleration due to gravity, m/s^2
g'	modified acceleration due to gravity, m/s^2 $\left(g' = \frac{\rho_0 - \rho_a}{\rho_a} g\right)$
ρ_0	effluent density, kg/m^3
ρ_a	density of ambient, kg/m^3
Q_0	discharge initial volume flux, m^3/s $(=u_0.h_0.b_0)$
M	discharge momentum flux $(=u_0.Q_0)$
B_0	discharge buoyancy flux $(=g'.Q_0)$
Fr_0	discharge Froude number $\left(= \frac{u_0}{\sqrt{g.d}}\right)$
Fr_d	discharge densimetric Froude number $\left(= \frac{u_0}{\sqrt{g'.d}}\right)$
Re	Reynolds number $\left(= \frac{u_0.d}{\upsilon}\right)$
υ	kinematic viscosity (m^2/s)
L_Q	discharge length scales, m $\left(L_Q = \frac{Q_0}{M_0^{1/2}}\right)$
L_M	jet to plume length scale, m $\left(L_M = \frac{M_0^{3/4}}{B_0^{1/2}}\right)$
x_p	location of plunge point, m
x_i	the location of impact point, m
x_m	the location of end of the initial mixing, m
χ	a linear geometric property of jet, m
S	waste filed dilution $\left(= \frac{C_0 - C_a}{C - C_a}\right)$
S_m	dilution at the end of the initial mixing zone
S_i	dilution at impact point
b_v	jet width in vertical plane, m $\left(= \frac{1}{e} I_{\max}\right)$
C	flow conductivity in arbitrary point, ms
C_0	conductivity of discharged flow, ms
C_a	conductivity of ambient water, ms
C_i	flow conductivity at impact point, ms
C_m	profile maximum conductivity, ms
I	Light Intensity
I_c	flow centerline intensity
$I_{\max}$	profile maximum intensity

References

Abdelwahed, M.S.T., Chu, V.H., 1981. Surface Jets and Surface Plumes in Cross-flows. Technical Report No. 81–1. Fluid Mechanics Laboratory, McGill University, Montreal.

Ahmed, M., Shayya, W., Hoey, D., Al-Handaly, J., 2001. Brine disposal from reverse osmosis desalination plants in Oman and the United Arab Emirates. J. Desalin. 133, 135–147.

Albertson, M.L., Dai, Y.B., Jensen, R.A., Rouse, H., 1949. Diffusion of submerged jets. Am. Soc. Civil Eng., Proc. 75 (10), 1541–1548.

Amon, R.M.W., Benner, R., 1998. Seasonal patterns of bacterial abundance and production in the Mississippi River plume and their importance for the fate of enhanced primary production. FEMS Microbiol. Ecol. 35 (3), 289–300.

Baines, W.D., Turner, J.S., Campbell, I.H., 1990. Turbulent Fountains in an open chamber. J. Fluid Mech. 212, 557–592.

Bandas, J., Bleninger, T., Socolofsky, S., 2008. Identification, Illustration, and Preliminary Measurements for Dense Discharges in a Cross Flow and Sloping Environment. Zachry Department of Civil Engineering, Texas A&M University and Institute for Hydromechanics, University of Karlsruhe.

Please cite this article in press as: Abessi, O., et al., Surface discharge of negatively buoyant effluent in unstratified stagnant water, Journal of Hydro-environment Research (2012), doi:10.1016/j.jher.2012.05.004

Bleninger, T., Jirka, G.H., 2008. Modeling and environmentally sound management of brine discharge from desalination plants. J. Desalin. 221, 585–597.

Bleninger, T., Niepelt, A., Jirka, G.H., 2010. Desalination plant discharge calculator. Desal. Water Treat. 13, 156–173. doi: 10.5004.

Capp, S.P., 1983. Experimental Investigation of the Buoyant Axisymmetric Jet. University of Buffalo, State University of New York, Buffalo.

Chu, V.H., Jirka, G.H., 1986. Surface Buoyant Jets. Encyclopedia of Fluid Mechanics, Chap. 25. Gulf, Houston.

Cipollina, A., Brucato, A., Grisafi, F., Nicosia, S., 2005. Bench-scale investigation of inclined dense jets. J. Hydr. Eng. 131 (11), 1017–1022.

Davidson, M.J., Pun, K.L., 2000. Locating discharge trajectories in still and moving ambient fluids. J. Hydr. Eng. 126 (7), 513–524.

Doneker, R.L., Jirka, G.H., 1997. D-CORMIX Continuous Dredge Disposal Mixing Zone Water Quality Model Laboratory and Field Data Validation Study. Oregon Graduate Institute, Portland, Ore, pp. 44.

Einav, R., Lokiec, F., 2003. Environmental aspects of a desalination plant in Ashkelon. J. Desalin. 156, 79–85.

Fan, L.N., 1967. Turbulent Buoyant Jets into Stratified or Flowing Ambient Fluids, Report No. KH-R-15. W.M. Keck Laboratory of Hydrology and Water Resources, California Institute of Technology, Pasadena, CA.

Fischer, B., List, J.E., Imberger, J., Brooks, H.N., 1979. Mixing in Inland and Coastal Waters. Academic Press, INC. San Diego, California.

Gholamreza-Kashi, S., Robert, J., Martinuzzi, Baddour, R.E., 2007. Mean flow field of a non buoyant rectangular surface jet. J. Hydr. Eng. 133 (2), 234–239.

Hansen, J., Schroder, H., 1968. Horizontal jet dilution studies by use of radioactive isotopes. Acta Polytechnica Scandinavia, Civil Eng. Build. Construction Ser. No. 49 (Copenhagen).

Hashim, A., Hajjaj, M., 2005. Impact of desalination plants fluid effluents on the integrity of seawater, with the Arabian Gulf in perspective. J. Desalin. 182, 373–393.

James, W.P., Vergara, I., Kim, K., 1983. Dilution of a dense vertical jet. J. Environ. Eng. 109 (6), 1273–1283.

Jirka, G., Adams, E., Stolzenbach, K., 1981. Properties of surface buoyant jets. J. Hydr. Div. 106 (HY11)

Jirka, G., 2004. Integral model for turbulent buoyant jets in unbounded stratified flows. Part I: single round jet. J. Environ. Fluid Mech. 4, 1–56.

Jirka, G.H., 2006. Integral model for turbulent buoyant jets in unbounded stratified flows Part 2: plane jet dynamics resulting from multiport diffuser jets. J. Environ. Fluid Mech. 6 (1), 43–100.

Jirka, G.H., 2007a. Buoyant surface discharges into water bodies. II: jet integral model. J. Hydr. Eng. 133 (9), 1021–1036.

Jirka, H.G., 2008. Improved discharge configurations for brine effluents from desalination plants. J. Hydr. Eng. 134 (1), 116–120.

Jones, G.R., Nash, J.D., Jirka, G.H., 1996. CORMIX3: An Expert System for Mixing Zone Analysis and Prediction of Buoyant Surface Discharges. Technical Rep. DeFrees Hydraulics Laboratory, Cornell Univ., Ithaca, N.Y (also published by Office of Water, Washington, D.C).

Jones, G., Nash, D., Doneker, L., Jirka, H., 2007. Buoyant surface discharge into water bodies. I: flow classification and prediction methodology. J. Hydr. Eng. 133 (9), 1010–1020.

Kassem, A., Jasim, I., Jamil, A.K., 2003. Three-dimensional modeling of negatively buoyant flow in diverging channels. J. Hydr. Eng. 129 (12), 936–947.

Kikkert, G.A., 2006. Buoyant jets with two- and three-dimensional trajectories. Ph.D. thesis, University of Canterbury, Christchurch, New Zealand.

Kikkert, G., Davidson, J., Noles, I., 2007. Inclined negatively buoyant discharges. J. Hydr. Eng. 133 (5), 545–554.

Law, A., Ho, W., Monismith, S., 2004. Double diffusive effect on desalination discharge. J. Hydr. Eng. 130 (5), 450–457.

Lee, J.H.W., Chu, V.H., 2003. Turbulent Jets and Plumes, a Lagrangian Approach. Kluwer Academic Publishers ASCE, Norwell, Massachusetts, USA, ISBN 1-4020-7520-0, pp. 390.

Liseth, P., 1970. Mixing of Merging Buoyant Jets from a Manifold in Stagnant Receiving Water of Uniform Density. Hydraulic Engineering Laboratory, College of Engineering, University of California, Berkeley.

Lattemann, S., Hoepner, T., 2003. Seawater Desalination-Impacts of Brine and Chemical Discharges on the Marine Environment. Desalination Publications, L'Aquila, Italy, pp. 142.

Lattemann, S., Hoepner, T., 2008. Environmental impact and impact assessment of seawater desalination. J. Desalin. 220, 1–15.

McLellan, T.N., Randal, R.E., 1986. Measurement of brine jet height and dilution. J. Waterway Port Coastal Ocean Eng. 112, 200–216.

Millero, J., Poisson, A., 1981. International one atmosphere equation of state for sea water. J. Deep Sea Res. 13, 453–459.

Nash, J.D., Jirka, G.H., 1996. Buoyant surface discharges into unsteady ambient flows. J. Dyn. Atmos. Oceans 24 (1–4), 75–84.

Nokes, R., 2008. Image Stream Version 7.00, User's Guide. Department of Civil and Natural Resources Engineering University of Canterbury, Christchurch, NZ.

Purnama, A., Al-Barwani, H.H., 2004. Some criteria to minimize the impact of brine discharge in to the sea. J. Desalin. 171, 167–172.

Rosler, R.S., Bankoff, S.G., 1963. Large scale turbulence characteristics of a submerged water jet. A.I.Ch.E. J. 9 (5), 672–676.

Roberts, P.J.W., Tome, G., 1987. Inclined dense jets in flowing current. J. Hydr. Eng. 113 (3), 323–341.

Roberts, P.J.W., Ferrier, A., Daviero, G., 1997. Mixing in inclined dense jet. J. Hydr. Eng. 123 (8), 693–699.

Safrai, I., Zask, A., 2008. Reverse osmosis desalination plants-marine environmentalist regular point of view. J. Desalin. 220, 72–84.

Shao, D., Law, A.W.K., 2010. Mixing and boundary interactions of 30° and 45° inclined dense jets. J. Environ. Fluid Mech. 10, 521–553. doi:10.1007/s10652-010-9171-2.

Sharp, J.J., Vyas, B.D., 1977. The buoyant wall jet. Proc. Inst. Civil Eng. 63 (2), 593–611.

Turner, J.S., 1966. Jets and plumes with negative or reversing buoyancy. J. Fluid Mech. 26, 779–792.

Wang, H., Law, A.W.K., 2002. Second-order integral model for a round buoyant jet. J. Fluid Mech. 459, 397–428.

Wright, S.J., 1984. Buoyant jets in density-stratified cross flow. J. Hydr. Eng. 110 (5), 643–656.

Xiao, J., Travis, J.R., Breitung, W., 2009. Non-Boussinesq integral model for horizontal turbulent buoyant round jets. J. Sci. Technol. Nucl. Install., 1–7. doi:10.1155/2009/862934.

Zeitoun, M.A., Reid, R.O., McHilhenny, W.F., Mitchell, T.M., 1972. Model Studies of Ocean Outfall Systems for Desalination Plants. Office of Saline Water, U.S. Department of the Interior, Washington D.C.

Zhang, H., Baddour, E., 1998. Maximum penetration of vertical round dense jets at small and large froud numbers. J. Hydr. Eng. 124 (5), 550–553.

Zhang, J.B., Chu, V.H., 2003. Shallow turbulent flows by video imaging method. J. Eng. Mech. 129 (10), 1164–1172.

Please cite this article in press as: Abessi, O., et al., Surface discharge of negatively buoyant effluent in unstratified stagnant water, Journal of Hydro-environment Research (2012), doi:10.1016/j.jher.2012.05.004